

Non-Markovian quantum Brownian motion in one dimension in electric fieldsH. Z. Shen,^{1,2} S. L. Su,³ Y. H. Zhou,⁴ and X. X. Yi^{1,2,*}¹*Center for Quantum Sciences and School of Physics, Northeast Normal University, Changchun 130024, China*²*Center for Advanced Optoelectronic Functional Materials Research, and Key Laboratory for UV Light-Emitting Materials and Technology of Ministry of Education, Northeast Normal University, Changchun 130024, China*³*School of Physics and Engineering, Zhengzhou University, Zhengzhou 450001, China*⁴*Quantum Information Research Center, Shangrao Normal University, Shangrao 334000, China*

(Received 7 December 2017; revised manuscript received 27 February 2018; published 24 April 2018)

Quantum Brownian motion is the random motion of quantum particles suspended in a field (or an effective field) resulting from their collision with fast-moving modes in the field. It provides us with a fundamental model to understand various physical features concerning open systems in chemistry, condensed-matter physics, biophysics, and optomechanics. In this paper, without either the Born-Markovian or rotating-wave approximation, we derive a master equation for a charged-Brownian particle in one dimension coupled with a thermal reservoir in electric fields. The effect of the reservoir and the electric fields is manifested as time-dependent coefficients and coherent terms, respectively, in the master equation. The two-photon correlation between the Brownian particle and the reservoir can induce nontrivial squeezing dynamics to the particle. We derive a current equation including the source from the driving fields, transient current from the system flowing into the environment, and the two-photon current caused by the non-rotating-wave term. The presented results then are compared with that given by the rotating-wave approximation in the weak-coupling limit, and these results are extended to a more general quantum network involving an arbitrary number of coupled-Brownian particles. The presented formalism might open a way to better understand exactly the non-Markovian quantum network.

DOI: [10.1103/PhysRevA.97.042121](https://doi.org/10.1103/PhysRevA.97.042121)**I. INTRODUCTION**

Quantum systems are never completely isolated from their external environments, which leads to decoherence that destroys the quantum coherence of the quantum system. Employing the effect of decoherence has recently become a key task for practical implementations of quantum information processing based on nanoscale solid-state materials [1,2], where the decoherence is mainly dominated by non-Markovian dynamics due to strong backactions from the environment. A fundamental issue is how to accurately take into account non-Markovian memory effects, which has attracted considerable attention in recent years both in theory [3–5] and in experiments [6–8].

Open quantum system dynamics can be described by a master equation for the reduced density matrix of the system. The master equation is usually derived based on the Born-Markovian (BM) approximation [9–12]. General treatments beyond those approximations did not appear until the studies of Wigner functions by Haake and Reibold [13], who addressed the issue in low-temperature and strong damping regimes. An exact non-Markovian master equation for Brownian motion was later derived by Hu, Paz, and Zhang [14], who employed the path-integral approach [15–17] for initially factorizable states. The exact master equation for a damped harmonic oscillator at finite temperature was reproduced later in Ref. [18] with non-Markovian quantum trajectories based on the stochastic Schrödinger equation. With this merit, many master equations

have been derived with fermion and boson systems as the environment [19–27].

The rotating-wave approximation (RWA) is widely used in quantum optics, which neglects the rapidly oscillating counter-rotating terms and the system Hamiltonian becomes time independent or depends slightly on time in the rotating frame. With recent developments in the area of circuit and cavity QED systems [28], ultra- and deep-strong light-matter couplings became experimentally achievable. This makes it necessary to take the counter-rotating terms into account. In fact, recent studies show that the counter-rotating terms in system-reservoir coupling play an important role in non-Markovian effects.

Previous studies of the exact non-Markovian master equation for quantum Brownian motion were mainly based on two models and/or methods. One is a system reservoir in a strong-coupling regime without external driving fields. This method includes the approach with a characteristic function [29], an adjoint master equation based on the Heisenberg picture [30], the Lindblad master equation [31], the momentum coupling model [32], and the Heisenberg-Langevin equation [33]. The other is of driven system-reservoir coupling in the rotating-wave approximation [34]. Although much progress has been made in this field, the derivation of the exact master equation for a quantum Brownian particle in the strong-coupling regime driven by an external field remains untouched so far.

In this paper, considering a charged-Brownian particle in one dimension in electric fields that couples to a thermal reservoir, we derive an exact non-Markovian master equation without the Born-Markovian and rotating-wave approxima-

*yixx@nenu.edu.cn

tion. We will show that the non-Markovian dynamics is completely determined by two coupled Green's functions, which contain all the environmental backactions on the system. We derive a non-Markovian master equation for the Brownian particle, whose dynamics contains not only coherent parts but also squeezing terms not achieved under the RWA. We derive a conserved-current equation including a source coming from the driving fields, transient current from the system flow into the environment, and a two-photon current attributed to the non-rotating-wave term. Finally, we generalize the results to open systems consisting of many-body coupled charged-Brownian particles in a thermal reservoir.

The remainder of this paper is structured as follows. In Sec. II, we present a model to describe the system under study, and give the evolution equation for operators of the system. In Sec. III, we derive a non-Markovian master equation for the Brownian particle. In Sec. IV, we discuss the effect of an initially correlated thermal equilibrium state on the dynamics. In Sec. V, we derive a current equation and discuss its properties. In Sec. VI, the time evolution of the position and momentum is discussed. In Sec. VII, we make comparisons between our method and the approximate method. In Sec. VIII, we generalize these results to a more general quantum network. Discussions and conclusions are given in Sec. IX.

II. NON-MARKOVIAN DYNAMICS IN THE HEISENBERG PICTURE

A. Model

We begin by considering a heavy, spinless particle of mass M_0 with charge $+q$ coupled to spinless and chargeless particles of mass m_k ($m_k \ll M_0$). Let \hat{X} be the coordinate of the Brownian particle, and \hat{x}_k the coordinate of the k th particle. The whole system is put in a box (see Fig. 1). In the absence of any external field, such a system can be described by the Hamiltonian

$$\hat{H} = \hat{H}_S + \hat{H}_R + \hat{H}_{SR}, \quad (1)$$

with

$$\hat{H}_S = \frac{\hat{P}^2}{2M_0} + \frac{1}{2}M_0\omega_c\hat{X}^2,$$

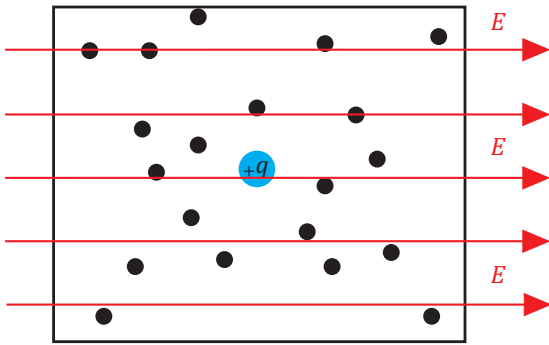


FIG. 1. Model for a charged-Brownian oscillator (charge is $+q$) linearly coupled to many harmonic oscillators in an electric field $E(t)$. The blue circle with $+q$ represents the charged-Brownian oscillator, which is coupled to a large number of oscillators [called the environment (small black circle) in later discussions].

$$\begin{aligned} \hat{H}_R &= \sum_k \frac{\hat{p}_k^2}{2m} + \frac{1}{2}m_k\omega_k\hat{x}_k^2, \\ \hat{H}_{SR} &= \sum_k G_k\hat{x}_k\hat{X}, \end{aligned} \quad (2)$$

where the first equation is the free Hamiltonian of the Brownian oscillator (particle) with frequency ω_c . The second term describes a general non-Markovian reservoir which is modeled as a collection of infinite oscillators (photonic modes), where \hat{b}_k^\dagger and \hat{b}_k are the corresponding creation and annihilation operators of the k th photonic mode with frequency ω_k and mass m_k , respectively, of the k th reservoir mode. \hat{X} and \hat{P} (\hat{q}_k and \hat{p}_k) are the Brownian oscillator (k th reservoir mode) position and momentum operators, and G_k are the reservoir-particle coupling constants.

In the presence of an external electric field $E(t)$, the total Hamiltonian becomes $\hat{H}_T = \hat{H} + qE'(t)\hat{X}$, where the electric field $E(t)$ can be taken as a plane wave $E'(t) = E \cos(\omega_e t)$. In this paper, we expand $qE'(t)\hat{X}$ to a more general form $\hbar E(t)\hat{a}^\dagger + \hbar E^*(t)\hat{a}$, which includes both RWA [$E(t)$ is a real function] and non-RWA [$E(t)$ is an imaginary function] terms. With this setting, the total Hamiltonian can be written as

$$\hat{H}_T(t) = \hat{H} + \hbar E(t)\hat{a}^\dagger + \hbar E^*(t)\hat{a}, \quad (3)$$

with $\hat{a} = \hat{X}/\sqrt{2\hbar/M_0\omega_c} - i\hat{P}/\sqrt{2\hbar M_0\omega_c}$.

B. Non-Markovian dynamics in the Heisenberg picture

We shall use the equation of motion in the Heisenberg picture to solve the dynamics of the Brownian particle under the effect of the reservoir. The time evolution of the Brownian particle annihilation operator $\hat{a}(t) = U^\dagger(t)\hat{a}(0)U(t)$, $\hat{b}_k(t) = U^\dagger(t)\hat{b}_k(0)U(t)$, with $\hat{b}_k = \hat{x}_k/\sqrt{2\hbar/m_k\omega_k} - i\hat{p}_k/\sqrt{2\hbar m_k\omega_k}$, where $U(t) = \mathcal{T}e^{-\frac{i}{\hbar}\int_0^t \hat{H}_T(\tau)d\tau}$ with the operator \mathcal{T} describes the chronological time ordering. It orders any product of operators such that the time argument increases from right to left. With the above transformation, Eq. (1) can be rewritten as

$$\hat{H} = \hbar\omega_c\hat{a}^\dagger\hat{a} + \sum_k \hbar\omega_k\hat{b}_k^\dagger\hat{b}_k + \sum_k \hbar\tilde{G}_k(\hat{a} + \hat{a}^\dagger)(\hat{b}_k + \hat{b}_k^\dagger), \quad (4)$$

where the effective coupling strength $\tilde{G}_k = G_k/\sqrt{4m_k M_0\omega_c\omega_k}$. In the Heisenberg picture, the system operator and environment operator obey

$$\begin{aligned} \frac{d}{dt}\hat{a}(t) &= -\frac{i}{\hbar}[\hat{a}(t), \hat{H}_H(t)] \\ &= -i\omega_c\hat{a}(t) - i\sum_k \tilde{G}_k[\hat{b}_k(t) + \hat{b}_k^\dagger(t)] - iE(t), \quad (5) \\ \frac{d}{dt}\hat{b}_k(t) &= -i\omega_k\hat{b}_k(t) - i\tilde{G}_k[\hat{a}(t) + \hat{a}^\dagger(t)], \quad (6) \end{aligned}$$

where $\hat{H}_H(t) = U^\dagger(t)\hat{H}_T(t)U(t)$. Solving Eq. (6) for $\hat{b}_k(t)$, we obtain

$$\hat{b}_k(t) = \hat{b}_k(0)e^{-i\omega_k t} - i\int_0^t \tilde{G}_k[\hat{a}(\tau) + \hat{a}^\dagger(\tau)]e^{-i\omega_k(t-\tau)}d\tau. \quad (7)$$

Substituting Eq. (7) into Eq. (5), we obtain a closed form of $\hat{a}(t)$,

$$\frac{d}{dt}\hat{a}(t) = -i\omega_c\hat{a}(t) - i[\hat{\mathcal{B}}(t) + \hat{\mathcal{B}}^\dagger(t)] - \int_0^t d\tau[\hat{a}(\tau) + \hat{a}^\dagger(\tau)]\mathcal{K}(t-\tau) - iE(t), \quad (8)$$

where the environment operator $\hat{\mathcal{B}}(t) = \sum_k \tilde{G}_k \hat{b}_k(0)e^{-i\omega_k t}$ and $\mathcal{K}(\tau) = f(\tau) - f^*(\tau) = -2i \sum_k \tilde{G}_k^2 \sin \omega_k \tau \equiv -2i \int J(\omega) \sin \omega \tau$ with $f(t) = \sum_k \tilde{G}_k^2 e^{-i\omega_k t}$, where $J(\omega) = \sum_k \frac{G_k^2}{4m_k M_0 \omega_k} \delta(\omega - \omega_k)$ is the spectral density of the reservoir. Because of the linearity of Eq. (8), the Brownian particle operator $\hat{a}(t)$ can be expressed, in terms of the initial field operators $\hat{a}(0)$ and $\hat{b}_k(0)$ of the Brownian particle and the reservoir, as

$$\hat{a}(t) = \mathcal{N}(t)\hat{a}(0) + \mathcal{M}(t)\hat{a}^\dagger(0) + \hat{\mathcal{P}}(t), \quad (9)$$

where the time-dependent coefficients can be obtained by substituting Eq. (9) into Eq. (8),

$$\begin{aligned} \dot{\mathcal{N}}(t) &= -i\omega_c \mathcal{N}(t) - \int_0^t d\tau [\mathcal{N}(\tau) + \mathcal{M}^*(\tau)]\mathcal{K}(t-\tau), \\ \dot{\mathcal{M}}(t) &= -i\omega_c \mathcal{M}(t) - \int_0^t d\tau [\mathcal{N}^*(\tau) + \mathcal{M}(\tau)]\mathcal{K}(t-\tau), \\ \dot{\hat{\mathcal{P}}}(t) &= -i\omega_c \hat{\mathcal{P}}(t) - \int_0^t d\tau [\hat{\mathcal{P}}(\tau) + \hat{\mathcal{P}}^\dagger(\tau)]\mathcal{K}(t-\tau) \\ &\quad - i[\hat{\mathcal{B}}(t) + \hat{\mathcal{B}}^\dagger(t)] - iE(t), \end{aligned} \quad (10)$$

subjected to the initial conditions $\mathcal{N}(0) = 1$, $\mathcal{M}(0) = 0$, and $\hat{\mathcal{P}}(0) = 0$. The integrodifferential equation (10) shows that $\mathcal{M}(t)$ and $\mathcal{N}(t)$ are just the propagating functions of the Brownian particle (the retarded Green's function in nonequilibrium Green's function theory [35]). In addition, $\hat{\mathcal{P}}(t)$ is, in fact, an operator coefficient and its solution can be obtained analytically from the inhomogeneous equation (10),

$$\hat{\mathcal{P}}(t) = \hat{c}(t) + \mathcal{U}(t), \quad (11)$$

with the fluctuation and coherent terms, respectively,

$$\begin{aligned} \hat{c}(t) &= -i \int_0^t d\tau [\mathcal{N}(t-\tau) - \mathcal{M}(t-\tau)][\hat{\mathcal{B}}(\tau) + \hat{\mathcal{B}}^\dagger(\tau)], \\ \mathcal{U}(t) &= i \int_0^t d\tau [\mathcal{M}(t-\tau) - \mathcal{N}(t-\tau)]E_r(\tau) \\ &\quad - \int_0^t d\tau [\mathcal{M}^*(t-\tau) - \mathcal{N}(t-\tau)]E_i(\tau), \end{aligned} \quad (12)$$

where the real part $E_r(t)$ and imaginary part $E_i(t)$ can be defined in Eq. (A10). Clearly, the first term $\hat{c}(t)$ and the second term $\mathcal{U}(t)$ of Eq. (11) are the influence of the environment and the electric field on the system dynamics, respectively. Physically, from the point of view of the Brownian particle, the electric field and environment are regarded as the two external "environments." One is that the electric field coherently drives the Brownian particle, while the other is that the environment causes the system to dissipate.

Detailed derivations of Eq. (11) can be found in the Appendix. From Eqs. (8)–(11) we can determine the exact

non-Markovian dynamics of the Brownian particle coupled to a general reservoir with an arbitrary time-dependent electric field, upon a given initial state $\rho_{SR}(0)$ of the total system. In the Heisenberg picture, quantum states are time independent. Once $\rho_{SR}(0)$ is given, the time evolution of any physical observable can be obtained directly from Eqs. (8)–(11) through the identity

$$\text{Tr}_{SR} \left[\frac{d\hat{\chi}(t)}{dt} \rho_{SR}(0) \right] \equiv \text{Tr}_S \left[\hat{\chi}(0) \frac{d\rho_S(t)}{dt} \right], \quad (13)$$

where $\hat{\chi}(t)$ is a function of $\hat{a}(t)$ and $\hat{a}^\dagger(t)$, i.e., $\hat{\chi}(t) = \sum_{N_1, N_2=0}^{\infty} \hat{a}(t)^{\dagger N_1} \hat{a}(t)^{N_2} \equiv \sum_{N_1, N_2=0}^{\infty} \hat{\chi}_{N_1 N_2}(t)$. The system density matrix operator $\rho_S(t) = \text{Tr}_R \rho_{SR}(t)$ with $\rho_{SR}(t) = U(t)\rho_{SR}(0)U^\dagger(t)$ that denotes the density matrix of the whole system, and $\text{Tr}_{SR} \equiv \text{Tr}_S \text{Tr}_R$ denotes traces over the system and environment, respectively. For example, the time evolution of the expectation values $\chi_{01}(t) = \langle \hat{a}(t) \rangle$, $\chi_{11}(t) = \langle \hat{a}^\dagger(t)\hat{a}(t) \rangle$, and $\chi_{02}(t) = \langle \hat{a}(t)\hat{a}(t) \rangle$ describe the Brownian particle amplitude, the Brownian particle intensity, and the two-photon correlation of the Brownian particle, respectively. From Eq. (9), we can obtain an equation set of $\chi_{01}(t)$, $\chi_{02}(t)$, $\chi_{11}(t)$ as follows,

$$\begin{aligned} \frac{d}{dt}\chi_{01}(t) &= A(t)[\chi_{01}(t) - \mathcal{U}] + B(t)[\chi_{01}^*(t) - \mathcal{U}^*] + \dot{\mathcal{U}}(t), \\ \frac{d}{dt}\chi_{02}(t) &= 2A(t)\chi_{02}(t) + 2B(t)\chi_{11}(t) + 2\chi_{01}(t)[\dot{\mathcal{U}} - A(t)\mathcal{U} \\ &\quad - B(t)\mathcal{U}^*] + \frac{d}{dt}\langle \hat{c}^2 \rangle - 2A(t)\langle \hat{c}^2 \rangle \\ &\quad - B(t)\langle \hat{c}\hat{c}^\dagger + \hat{c}^\dagger\hat{c} \rangle + B(t), \\ \frac{d}{dt}\chi_{11}(t) &= \frac{\dot{\mathcal{F}}}{\mathcal{F}}\langle \hat{\chi}_{11}(t) - \hat{c}^\dagger\hat{c} \rangle + \frac{d}{dt}\langle \hat{c}^\dagger\hat{c} \rangle \\ &\quad + \{B^*(t)\langle \hat{\chi}_{02}(t) - \hat{c}^2 \rangle \\ &\quad + \chi_{01}^*(t)[\dot{\mathcal{U}} - A(t)\mathcal{U} - B(t)\mathcal{U}^*(t)] + \text{H.c.}\}, \end{aligned} \quad (14)$$

with

$$\begin{aligned} A(t) &= (\dot{\mathcal{N}}\mathcal{N}^* - \dot{\mathcal{M}}\mathcal{M}^*)/\mathcal{F}(t), \\ B(t) &= (\mathcal{N}\dot{\mathcal{M}} - \dot{\mathcal{N}}\mathcal{M})/\mathcal{F}(t), \\ \mathcal{F}(t) &= |\mathcal{N}(t)|^2 - |\mathcal{M}(t)|^2, \end{aligned} \quad (15)$$

where $\mathcal{M}(t)$ and $\mathcal{N}(t)$ are determined by Eq. (10).

Suppose the system and the environment are initially uncorrelated—the reservoir modeled by the Hamiltonian $\hat{H}_R = \sum_k \omega_k \hat{b}_k^\dagger \hat{b}_k$ is in a thermal equilibrium state, while the system is in a coherent state $|\alpha\rangle$. The reservoir is assumed to have a Gaussian (thermal) initial state,

$$\rho_{SR}(0) = \rho_S \otimes \rho_R, \rho_R = \frac{e^{-\beta \hat{H}_R}}{\text{Tr}_R e^{-\beta \hat{H}_R}}, \quad (16)$$

where $\rho_S = |\alpha\rangle\langle\alpha|$ can be obtained by defining it as an eigenstate of the annihilation operator a with an eigenvalue α , and $\beta = 1/\kappa_B T$ with κ_B the Boltzmann constant, and T the temperature of the reservoir. In this paper, we only focus on the case of zero temperature.

III. EXACT NON-MARKOVIAN MASTER EQUATION

A. Non-Markovian master equation for Brownian particle

We define $\hat{a}(t) = \hat{s}(t) + \hat{c}(t)$ with $\hat{s}(t) = \mathcal{N}(t)\hat{a}(0) + \mathcal{M}(t)\hat{a}^\dagger(0) + \mathcal{U}(t)$. We notice that the operator $\hat{s}(t)$ commutes with $\hat{c}(t)$ from Eq. (9). Therefore, for any normal product $\hat{\chi}_{N_1 N_2}(t) = \hat{a}(t)^{\dagger N_1} \hat{a}(t)^{N_2}$, we obtain

$$\hat{\chi}_{N_1 N_2}(t) = \sum_{m=0}^{N_1} \sum_{n=0}^{N_2} C_{N_1}^m C_{N_2}^n \hat{s}^{\dagger(N_1-m)} \hat{s}^{(N_2-n)} \hat{c}^{\dagger m} \hat{c}^n, \quad (17)$$

where the combination number $C_{N_1}^m = N_1! / m!(N_1 - m)!$. The non-Markovian effects of the environment on a Brownian particle are all incorporated into these terms $\hat{c}^{\dagger m} \hat{c}^n$, whose expansions yield

$$\begin{aligned} \hat{c}^{\dagger m} \hat{c}^n &= \int_0^t dt_1 \cdots \int_0^t dt_m \varphi^*(t - t_1) \cdots \varphi^*(t - t_m) \\ &\times \int_0^t d\tau_1 \cdots \int_0^t d\tau_n \varphi^*(t - \tau_1) \cdots \varphi^*(t - \tau_n) \\ &\times \tilde{B}(t_1) \tilde{B}(t_2) \cdots \tilde{B}(t_m) \cdot \tilde{B}(\tau_1) \tilde{B}(\tau_2) \cdots \tilde{B}(\tau_n), \end{aligned} \quad (18)$$

where $\varphi(t) = -i[\mathcal{N}(t) - \mathcal{M}(t)]$ and $\tilde{B}(t) = \hat{B}(t) + \hat{B}^\dagger(t)$.

For the considered system-reservoir interaction (4), the reservoir operators $\tilde{B}(t_i)$ satisfy the Gaussian statistics. That is, $(m+n)$ -time correlation functions vanish if n is odd. For even n , according to the Gaussian property, the terms up to second order in the reservoir correlation function are sufficient to exactly describe the dynamics of the system [36,37],

$$\langle \tilde{B}(t_1) \tilde{B}(t_2) \cdots \tilde{B}(t_{2m}) \rangle = \sum_{\text{pair } l_1, l_2} \prod \langle \mathcal{I}_+ \tilde{B}(t_{l_1}) \tilde{B}(t_{l_2}) \rangle, \quad (19)$$

where the index pairs denotes the division of the labels 1 to $2m$ into n unordered pairs. The operator \mathcal{I}_+ is the index ordering operator preserving the order of operators on the right-hand side of Eq. (19) similar to the left-hand side. Note that here we have applied a generalized Wick's theorem in the form of Wightman functions rather than the usual form with time-ordered correlation functions [38,39].

Under the factorized initial density matrix (16) guarantees that the Liouville operator is independent of the initial system state, which was also observed in Refs. [14–16]. The initial state (16) and the kernel in Eq. (17), both of which are of Gaussian form and result from the linearity of the total Hamiltonian, allow exact integration. This makes the reduced density matrix $\rho_S(t) = \text{Tr}_R[\rho_{SR}(t)]$ also a Gaussian. Together with the requirements of conservation of probability [$\text{Tr}(\rho_S) = 0$], Hermiticity ($\rho_S = \rho_S^\dagger$), and state-independent coefficients, we obtain the following form of a time-convolutionless master equation,

$$\begin{aligned} \dot{\rho}_S &= -i[\hat{H}_{\text{eff}}(t), \rho_S] \\ &+ \gamma_1(t)(2\hat{a}\rho_S\hat{a}^\dagger - \hat{a}^\dagger\hat{a}\rho_S - \rho_S\hat{a}^\dagger\hat{a}) \\ &+ \gamma_2(t)(\hat{a}\rho_S\hat{a}^\dagger + \hat{a}^\dagger\rho_S\hat{a} - \hat{a}^\dagger\hat{a}\rho_S - \rho_S\hat{a}^\dagger\hat{a}) \\ &+ [\gamma_3^*(t)(2\hat{a}\rho_S\hat{a} - \hat{a}\hat{a}\rho_S - \rho_S\hat{a}\hat{a}) + \text{H.c.}], \end{aligned} \quad (20)$$

where the time-dependent effective Hamiltonian

$$\hat{H}_{\text{eff}}(t) = \delta(t)\hat{a}^\dagger\hat{a} + [D(t)\hat{a}^2 + \phi(t)\hat{a} + \text{H.c.}], \quad (21)$$

To figure out the time coefficients in Eq. (20), we also can compute these physical observables $\chi_{01}(t)$, $\chi_{02}(t)$, and $\chi_{11}(t)$ from the master equation (20),

$$\begin{aligned} \frac{d}{dt} \chi_{01}(t) &= -[\gamma_1(t) + i\delta(t)]\chi_{01}(t) - 2iD^*(t)\chi_{01}^*(t) - i\phi^*(t), \\ \frac{d}{dt} \chi_{02}(t) &= -4iD^*(t)\chi_{11}(t) - [2\gamma_1(t) + 2i\delta(t)]\chi_{02}(t) \\ &\quad - [2\gamma_3(t) + 2iD^*(t)] - 2i\phi^*(t)\chi_{01}(t), \\ \frac{d}{dt} \chi_{11}(t) &= \gamma_2(t) - 2\gamma_1(t)\chi_{11}(t) + \{2iD\chi_{02}(t) \\ &\quad + i\phi\chi_{01}(t) + \text{H.c.}\}. \end{aligned} \quad (22)$$

By comparing Eqs. (14) and (22), we can obtain the time coefficients as follows,

$$\begin{aligned} D(t) &= B^*(t)/2i, \quad \delta(t) = -\text{Im}[A(t)], \\ \phi(t) &= -i[\dot{\mathcal{U}}^*(t) - A^*(t)\mathcal{U}^*(t) - B^*(t)\mathcal{U}(t)], \\ \gamma_1(t) &= -\dot{\mathcal{F}}(t)/2\mathcal{F}(t), \\ \gamma_2(t) &= \left(\frac{d}{dt} - \frac{\dot{\mathcal{F}}(t)}{\mathcal{F}(t)}\right)\langle \hat{c}^\dagger \hat{c} \rangle - \{B^*(t)\langle \hat{c}^2 \rangle + \text{H.c.}\}, \\ \gamma_3(t) &= \left(A(t) - \frac{1}{2} \frac{d}{dt}\right)\langle \hat{c}^2 \rangle + \frac{B(t)}{2}\langle \hat{c}\hat{c}^\dagger + \hat{c}^\dagger\hat{c} \rangle, \end{aligned} \quad (23)$$

where $A(t)$, $B(t)$, and $\mathcal{F}(t)$ are given by Eq. (15). Below, we discuss the physical meaning of the time-dependent coefficients in the non-Markovian master equation (20) as follows:

(i) The first term in Eq. (21), with $\delta(t)$, accounts for the free dynamics of the Brownian particle, induced by frequency shifts owing to its coupling with the environment.

(ii) The second term in Eq. (21) denotes the two-photon process, originated from asymmetries in both position and momentum in the whole system. However, this term is small (equal exactly zero in the rotating-wave approximation), leading to a negligible squeezing effect in the weak-coupling regime.

(iii) The third term $\phi(t)$ in Eq. (21) is a coherent term, which denotes the effective driving to the system, where the renormalized driving $\phi(t)$ results from the backreaction between the electric field and reservoir.

(iv) $\gamma_1(t)$ in Eq. (20) is a dissipation (damping) rate, which drives the center of the Brownian wave packet towards its nonequilibrium stationary state induced by the reservoir.

(v) $\gamma_2(t)$ in Eq. (20) is the fluctuation (noise) coefficient due to the backreactions between the system and the reservoir.

(vi) $\gamma_3(t)$ in Eq. (20) is the squeezing rate, given by the counter-rotating terms $\hat{a}\hat{b}_k$ and $\hat{a}^\dagger\hat{b}_k^\dagger$ between the Brownian particle and the reservoir.

As we see, the first three terms of Eq. (20) have the standard form as the exact master equation for the system in Eq. (4) without the counter-rotating terms $\hat{a}\hat{b}_k$ and $\hat{a}^\dagger\hat{b}_k^\dagger$, but with the coefficients modified by them. The last two terms of Eq. (20) are contributed from the two-photon correlations $\hat{a}\hat{b}_k$ and $\hat{a}^\dagger\hat{b}_k^\dagger$ in the reservoir. Under the derived coefficients (23), we can check the identity (13) is valid for arbitrary operators $\hat{\chi}_{N_1 N_2}$. In addition, we also prove that Eq. (20) is correct by canceling the driving term in Eq. (3) with an unitary transformation $U_1(t) = e^{-ir(t)(\hat{a} + \hat{a}^\dagger)}$, where $r(t)$ is an arbitrary time-dependent real function.

The master equation (20) derived in this section is exact in which its solution is guaranteed to agree with the reduced state of a unitary dynamics of the universe, which is of a Gaussian class, completely positive, trace-preserving, non-Markovian dynamics in a charged-Brownian particle merged into an electric field and coupled with a thermal reservoir without invoking either the Born-Markovian or the rotating-wave approximation (RWA). It relies on two hypotheses: that the initial state of the universe is a product state and that the initial state of the reservoir is Gaussian.

B. The case of rotating-wave approximation

In many physical systems described by the Hamiltonian of Eq. (4), the typical coupling intensity \tilde{G}_k is many orders of magnitude smaller than the frequencies ω_k , characterizing the weak-coupling regime. It is then a good approximation to drop the counter-rotating terms ($\hat{a}b_k$ and $\hat{a}^\dagger\hat{b}_k^\dagger$), a procedure which is known as the rotating-wave approximation.

In this case, we can obtain the following master equation with the rotating-wave approximation by using similar methods to those used in the previous section,

$$\begin{aligned} \dot{\rho}(t) = & -i[\hat{H}_{\text{RWA}}(t), \rho] + \gamma_1(t)(2\hat{a}\rho\hat{a}^\dagger - \hat{a}^\dagger\hat{a}\rho - \rho\hat{a}^\dagger\hat{a}) \\ & + \gamma_2(t)(\hat{a}\rho\hat{a}^\dagger + \hat{a}^\dagger\rho\hat{a} - \rho\hat{a}^\dagger\hat{a} - \rho\hat{a}\hat{a}^\dagger), \end{aligned} \quad (24)$$

where $\hat{H}_{\text{RWA}}(t) = \delta(t)\hat{a}^\dagger\hat{a} + \phi(t)\hat{a} + \phi^*(t)\hat{a}^\dagger$.

Therefore, considering that the reservoir is initially in the thermal equilibrium state, the coefficients $\delta(t)$, $\gamma_1(t)$, and $\gamma_2(t)$ in the master equation can be uniquely determined and given by

$$\begin{aligned} \delta(t) &= -\text{Im}[\dot{u}(t)/u(t)], \quad \gamma_1(t) = -\text{Re}[\dot{u}(t)/u(t)], \\ \gamma_2(t) &= \dot{v} - [\dot{u}(t)/u(t) * v(t) + \text{c.c.}], \\ \phi(t) &= -i\dot{x}^*(t) + i[\dot{u}^*(t)/u^*(t)\dot{x}^*(t)], \end{aligned} \quad (25)$$

with the parameters satisfying

$$\begin{aligned} \dot{u} + i\omega_c u(t) + \int_0^t f(t-\tau)u(\tau)d\tau &= 0, \\ v(t) &= \int_{t_0}^t d\tau \int_0^t d\tau' u(t-\tau')\tilde{f}(\tau'-\tau)u^*(t-\tau), \\ x(t) &= -i \int_0^t E(\tau)u(t-\tau)d\tau, \end{aligned} \quad (26)$$

where $\tilde{f}(t-\tau)$ is the finite-temperature correlation function $\tilde{f}(t-\tau) = \int J(\omega)n(\omega)e^{-i\omega t}d\omega$ with environment mean photon number $n(\omega) = (e^{\hbar\beta\omega} - 1)^{-1}$ with $\beta = 1/\kappa_B T$, where κ_B is the Boltzmann constant, and T the temperature. Especially, $\gamma_2(t) = 0$ due to $n(\omega) = 0$ when $T = 0$.

For the quantum noise of Brownian motion, we consider an environment fluctuating according to a Gaussian Ornstein-Uhlenbeck stochastic process in a zero-temperature environment [40,41] characterized by its strength Γ and correlation time $1/\lambda$ as follows,

$$f(t-\tau) = 0.5\Gamma\lambda e^{-i\omega_c(t-\tau)-\lambda|t-\tau|}, \quad (27)$$

which has a clear boundary between Markovian and non-Markovian regimes [3,9]. More specifically speaking, the parameter λ is connected to the reservoir correlation time τ_b

by the relation $\tau_b \simeq \lambda^{-1}$, while the time scale τ_s , on which the state of the system changes, is given by $\tau_s \simeq \Gamma^{-1}$. In this sense, the boundary between Markovian regimes and non-Markovian regimes can be approximately specified by the ratio of $\tau_b/\tau_s = \Gamma/\lambda$. When Γ/λ is very small, which means that the reservoir correlation time τ_b is much smaller than the relaxation time of the quantum subsystem τ_s , the decoherence mechanics is Markovian. When Γ/λ is large, the memory effect of the reservoir should be taken into account and the dynamics of this open system is then non-Markovian. In fact, one can demonstrate that the coupled Green's-function equations in Eq. (10) reduce to the usual Markovian Lindblad-type master equation in the limit $\lambda \gg \max\{\Gamma, \omega_c\}$, due to the fact that the reservoir correlation function reduces to the Dirac δ function $f(t-\tau) \rightarrow \text{const} \delta(t-\tau)$ in this situation.

In Fig. 2, we show the two-photon term $D(t)$, coherent driving term $\phi(t)$, decay rate γ_1 , fluctuation (noise) coefficient γ_2 , and the squeezing rate γ_3 for Ornstein-Uhlenbeck correlation (27) in the weak- and strong-coupling cases with a comparison to the RWA. For a given coupling strength Γ , we find from the figure that the results given by the exact non-RWA given by Eq. (23) are in good agreement with those obtained by the exact RWA results given by Eq. (25) when the weak-coupling conditions are satisfied ($\Gamma = 0.05\omega_e \ll \omega_c = 5\omega$) [see Figs. 2(a)–2(j); in Figs. 2(f)–2(j), the spectral width of the environment is larger than the coupling strength γ , which approximately corresponds to the Markovian limit]. In this case, the contribution of the counter-rotating wave to the time coefficients is very small, i.e., the two-photon process $D(t)$, fluctuation (noise) coefficient γ_2 , and the squeezing rate γ_3 are close to zero. With an increase of Γ , $\Gamma = 5\omega_e \simeq \omega_c$ [see Figs. 2(l)–2(n)], the curve obtained by the RWA case decided by Eq. (25) has serious deviations from those obtained by the exact non-RWA results (23). The largest difference between the exact result and the RWA for a strong coupling is a significant manifestation of counter-rotating terms, where the two-photon process, fluctuation (noise) coefficient, and the squeezing rate are larger than this case in weak coupling.

IV. DISCUSSION ON THE INITIAL CORRELATED THERMAL EQUILIBRIUM STATE

In realistic situations, the Brownian particle is initially in a state correlated to the state of the reservoir as follows,

$$\rho_{SR}(0) = e^{-\beta\hat{H}}/\text{Tr}_{SR} e^{-\beta\hat{H}}, \quad (28)$$

with \hat{H} given by Eq. (1). Assume that the system-environment coupling is not so strong, such that we might expand the above initial state up to the first few orders in the coupling constant. The following equation will be used in the expansion,

$$e^{\theta(\hat{X}+\hat{Y})} = e^{\theta\hat{X}}\mathcal{T} \exp \left[\int_0^\theta e^{-\hat{X}\tau}\hat{Y}e^{\hat{X}\tau}d\tau \right], \quad (29)$$

where \mathcal{T} represents the time-ordered product, which orders any product of operators such that the time argument increases from right to left. By setting $\theta = \beta$, $\hat{X} = -\hat{H}_S - \hat{H}_R$, $\hat{Y} = -\varepsilon\hat{H}_{SR}$ [for discussion purposes, here we introduce ε , which denotes the dimensionless coupling strength; $\varepsilon = 1$ corresponds to Eq. (1) in the main text], we can expand the thermal equilibrium

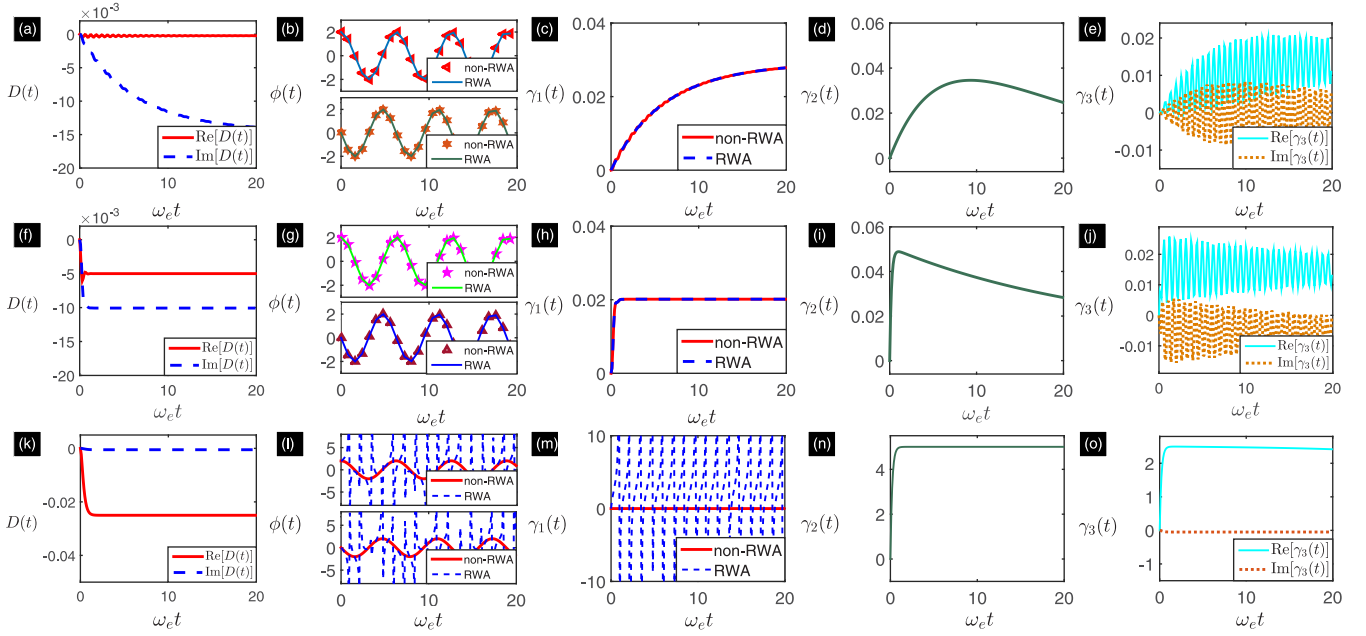


FIG. 2. Value of the time-dependent two-photon term $D(t)$, coherent driving term $\phi(t)$, decay rate $\gamma_1(t)$, fluctuation (noise) coefficient $\gamma_2(t)$, and the squeezing rate $\gamma_3(t)$ as a function of the time t with the Ornstein-Uhlenbeck correlation (27). The electric field takes the plane wave $E(t) = Ee^{-i\omega_e t}$. The parameters chosen are (top) $\omega_c = 5\omega_e$, $E = 2\omega_e$, $\Gamma = 0.05\omega_e$, $\lambda = 0.2\omega_e$; (middle) $\Gamma = 0.05\omega_e$, $\lambda = 5\omega_e$; (bottom) $\Gamma = 5\omega_e$, $\lambda = 10\omega_e$. Here and hereafter, ω_c , E , Γ , and \mathcal{U} are rescaled in units of ω_e , and the time t is then in units of $1/\omega_e$. Hence all parameters are dimensionless. Non-rotating-wave and rotating-wave results are given by numerically solving Eqs. (23) and (25), respectively.

state up to any order in the coupling constant ε ,

$$\begin{aligned}
 e^{-\beta\hat{H}} &= e^{-\beta\hat{H}_S - \beta\hat{H}_R} \left[1 + \sum_{j=1}^{\infty} (-\varepsilon)^j \int_0^{\beta} dt_1 \int_0^{t_1} dt_2 \right. \\
 &\quad \cdots \int_0^{t_{j-1}} dt_j \hat{H}_{SR}(-i\hbar t_1) \hat{H}_{SR}(-i\hbar t_2) \\
 &\quad \left. \cdots \hat{H}_{SR}(-i\hbar t_j) \right] \\
 &= e^{-\beta\hat{H}_S - \beta\hat{H}_R} \left[1 + \sum_{j=1}^{\infty} \hat{\eta}_j \right], \quad (30)
 \end{aligned}$$

where $\hat{H}_{SR}(t) = e^{\frac{i}{\hbar}(\hat{H}_S + \hat{H}_R)t} \hat{H}_{SR} e^{-\frac{i}{\hbar}(\hat{H}_S + \hat{H}_R)t}$, and

$$\begin{aligned}
 \hat{\eta}_j &= (-\varepsilon)^j \int_0^{\beta} dt_1 \int_0^{t_1} dt_2 \cdots \int_0^{t_{j-1}} dt_j \hat{H}_{SR}(-i\hbar t_1) \\
 &\quad \times \hat{H}_{SR}(-i\hbar t_2) \cdots \hat{H}_{SR}(-i\hbar t_j).
 \end{aligned}$$

The partition function is given by

$$\text{Tr}_{SR} e^{-\beta\hat{H}} = \{\text{Tr}_{SR} e^{-\beta\hat{H}_S - \beta\hat{H}_R}\} (1 + \mu_2 + \mu_3 + \mu_4),$$

with

$$\begin{aligned}
 \mu_j &= (-\varepsilon)^j \int_0^{\beta} dt_1 \int_0^{t_1} dt_2 \cdots \int_0^{t_{j-1}} dt_j \langle \hat{H}_{SR}(-i\hbar t_1) \\
 &\quad \times \hat{H}_{SR}(-i\hbar t_2) \cdots \hat{H}_{SR}(-i\hbar t_j) \rangle_{SR}, \quad (31)
 \end{aligned}$$

where $\rho_S = e^{-\beta\hat{H}_S} / \{\text{Tr}_S e^{-\beta\hat{H}_S}\}$, $\rho_R = e^{-\beta\hat{H}_R} / \{\text{Tr}_R e^{-\beta\hat{H}_R}\}$. $\langle \bullet \rangle_{SR}$ is denoted via $\text{Tr}_{SR} \{\bullet \rho_S \rho_R\}$. Therefore, Eq. (28) is written as

$$\rho_{SR}(0) = \rho_{SR}^{(0)}(0) + \varepsilon \rho_{SR}^{(1)}(0) + \varepsilon^2 \rho_{SR}^{(2)}(0) + \cdots, \quad (32)$$

where the first few order expansions are

$$\begin{aligned}
 \rho_{SR}^{(0)}(0) &= \rho_S \rho_R, \quad \rho_{SR}^{(1)}(0) = -\rho_S \rho_R \int_0^{\beta} d\beta_1 \hat{H}_{SR}(-i\hbar\beta_1), \\
 \rho_{SR}^{(2)}(0) &= \rho_S \rho_R \int_0^{\beta} d\beta_1 \int_0^{\beta_1} d\beta_2 \{ \hat{H}_{SR}(-i\hbar\beta_1) \\
 &\quad \times \hat{H}_{SR}(-i\hbar\beta_2) - \langle \hat{H}_{SR}(-i\hbar\beta_1) \hat{H}_{SR}(-i\hbar\beta_2) \rangle_{SR} \}, \quad (33)
 \end{aligned}$$

With Eq. (9) and the identity (13) as well as the correlated initial state (32), we can study the time-dependent non-Markovian dynamics for the Brownian particle when the system and environment are initially prepared in a correlated thermal equilibrium state. From the above results, we find that the first term in Eq. (32) represents the zero-order approximation, which corresponds to the uncorrelated initial state given by Eq. (16). This is valid for weak system-environment couplings limit. When the system-environment coupling is strong, we need to consider the influence of the high-order terms $\rho_{SR}^{(j)}(0)$ ($j \geq 1$) to the system dynamics. The other terms in Eq. (32) are high-order contributions to the initial dynamics.

From the analysis above, we can conclude that the initial dynamics can be treated well by the high-order terms, which is the correction to the zero-order term when the coupling strength becomes strong. Although our results have been limited to zero order, our conclusion is general. Namely, with an increase in coupling strength, we need to consider the higher-order contributions.

V. EXACT TRANSIENT CURRENT FOR QUANTUM TRANSPORT WITHOUT ROTATING-WAVE APPROXIMATION

The transient current from the system flow into the environment is defined in the Heisenberg picture as

$$I(t) = \frac{d}{dt} \langle \hat{N}(t) \rangle = -i \langle [\hat{N}(t), \hat{H}_H(t)] \rangle, \quad (34)$$

where $\hat{N}(t) = \sum_k \hat{b}_k^\dagger(t) \hat{b}_k(t)$. By explicitly calculating the above commutation relation with the Hamiltonian of Eq. (3) and then transforming it into the Schrödinger picture, we have a transient equation for conservation current,

$$\frac{\partial n(t)}{\partial t} = S(t) - I(t) + C(t), \quad (35)$$

where $n(t) = \text{Tr}_S[\hat{a}^\dagger \hat{a} \rho_S(t)]$ is the total exciton number in the Brownian particle, $S(t) = -i \text{Tr}_{SR}[E(t) \hat{a}^\dagger(t) - E^*(t) \hat{a}(t)]$ is the source coming from the driving fields, and $I(t)$ the transient current from the system flow into the environment, this defined term,

$$C(t) = 2i \text{Tr}_{SR} \sum_k \tilde{G}_k \hat{a}(t) \hat{b}_k(t) \rho_{SR}(0) + \text{H.c.}, \quad (36)$$

denotes the two-photon current from the non-rotating-wave term. Equation (35) tells us that the increase of the photon number in the resonators is equal to the photons received from the driving field and non-rotating-wave term minus the photon flow into the environment.

Now, we turn to the exact numerical calculation. We compare the above transient current in the weak-coupling limit ($\Gamma \ll \omega_c$) with the exact numerical solution of coherent driving sources, transient current, and the two-photon current from the non-rotating-wave term, respectively. In the numerical calculation, we take $E = 0.1\omega_e$, $E = \omega_e$, $E = 10\omega_e$. The result is plotted in Fig. 3 where the Brownian frequency $\omega_c = 10\omega_e$ and $\Gamma = 0.1\omega_e$ which belongs to a weak coupling and the RWA is applicable. As the electric field intensity increases, the amplitude of the current increases. From Figs. 3(a)–3(c), we find that in the weak-coupling limit, RWA is in good agreement with the exact solution, in particular, the coherence current $S(t)$ coming from the electric field source. This is because the coherence current $S(t) = -iE(t)[\alpha N(t) + \alpha^* M(t) + U(t)] + \text{c.c.}$ approaches the situation of RWA, where $\mathcal{N}(t) \rightarrow u(t)$, $\mathcal{M}(t) \rightarrow 0$. But the transient current $I(t)$ in RWA cannot witness a time oscillation with non-RWA [in this case, the physical mechanism originates from the transition paths; see the blue solid lines in Fig. 4(b)]. Nevertheless, it can still capture some useful information, which is consistent with the upper edge of the transient current in non-RWA. In the rotating-wave approximation, no two-photon current exists. In contrast, the case in non-RWA has a nonzero two-photon current $C(t)$, which originates from the terms containing $\hat{a} \hat{b}_k$ and $\hat{a}^\dagger \hat{b}_k^\dagger$ in Eq. (36). Therefore, the non-RWA parts in Eq. (36) are the contribution of the two-photon current $C(t)$, which usually generates pairs of photons. This is the other significance of the non-Markovian strong-coupling dynamics.

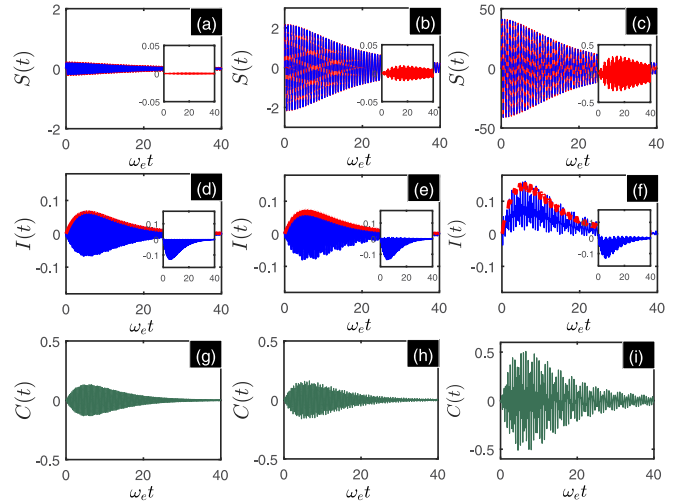


FIG. 3. Comparison of the Brownian particle currents in the exact numerical simulation (20) with rotating-wave approximation (24) with different electric field intensities. (a)–(c), (d)–(f), and (g)–(i) are current $S(t)$ coming from the electric field source, transient current $I(t)$ from the system flow into the environment, and the two-photon current $C(t)$ from the non-rotating-wave term, respectively, with the non-RWA solution (solid line) and the RWA solution (dashed line). The parameters chosen are $\omega_c = 10\omega_e$, $\Gamma = 0.1\omega_e$, $\lambda = 0.3\omega_e$, $E = 0.1\omega_e$ for (a), (d), and (g); $E = \omega_e$ for (b), (e), and (h); $E = 10\omega_e$ for (c), (f), and (i). The inset shows differences between non-RWA and RWA, i.e., $\Delta S(t) = S_{\text{non-RWA}}(t) - S_{\text{RWA}}(t)$, $\Delta I(t) = I_{\text{non-RWA}}(t) - I_{\text{RWA}}(t)$.

Next, we shall present an exact numerical simulation for different values of the coupling constants between the Brownian particle and the thermal reservoir, to examine the different non-Markovian dynamics in the weak-coupling and the strong-coupling regime. Figure 5 shows the field amplitude of Eq. (9) with different coupling strengths and different Brownian particle frequencies. In the weak-coupling regime, the behavior of the field amplitude depends highly on the ratio of Γ to ω_c . When the coupling strength is much smaller than the Brownian particle frequency ω_c (see Fig. 5), the field amplitude dampens to zero. When the Brownian particle frequency ω_c turns down to ω_e , the field amplitude increases gradually to a steady value with small oscillations. These numerical results agree with the RWA solution, as shown in Figs. 5(a)–5(d). In the strong-coupling regime, the field amplitude keeps oscillating without decay in both cases, where the case on RWA has very large derivations with that in non-RWA [see Figs. 5(e) and 5(f)]. The absence of damping (dissipation) is totally due to the effect of the counter-rotating terms and non-Markovian contributions, where counter-rotating terms make the main contribution to the system dynamics [the term $\hat{a} \hat{b}_k$ and coherent term $E(t)$ reach dynamical equilibrium, whereas $\hat{a}^\dagger \hat{b}_k^\dagger$ allows an unlimited increase in the number of excitations in the system]. Thus we can confirm that this process is predominantly a two-photon process. The complicated oscillating behavior [see Figs. 5(e) and 5(f)] is an interference effect between the coherence electric field and the coupling between the Brownian particle and reservoir.

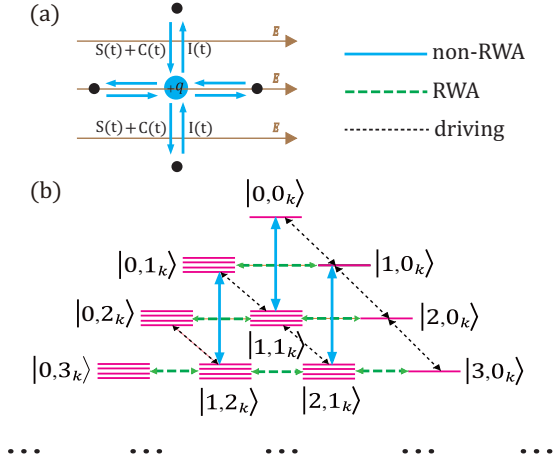


FIG. 4. (a) In the framework of a factorized direct product of the system and the environment Gaussian state, the conserved currents connected with each part are established. (b) Energy diagram showing the zero-, one-, and two-exciton states $\dots m_k + n$ exciton states $|n, m_k\rangle$ (n excitons in the Brownian particle, m_k photons in k th mode for the environment), and the transition paths: Blue solid lines with arrows denote two-exciton transitions (non-RWA processes), green dashed lines with arrows denote converted exciton conversion (RWA processes), and black dotted lines with arrows denote coherent driving sources (coherent processes).

VI. TIME EVOLUTION OF THE POSITION AND MOMENTUM

The advantage of having solved the equations of motion in the Heisenberg picture is that they easily allow us to compute the expected values of relevant operators. The expectation values for \hat{q} and \hat{p} follow straightforwardly

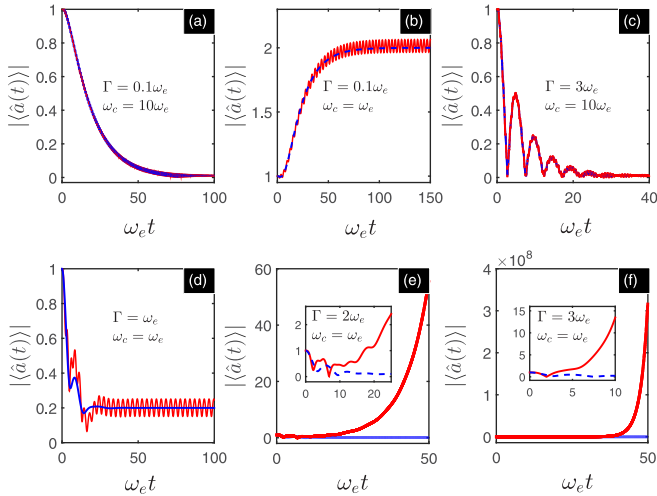


FIG. 5. The time evolution of the Brownian particle field amplitude with different coupling strengths and free frequency of the Brownian particle. The figure shows the differences in the non-rotating-wave and rotating-wave situations. The parameters chosen are $\alpha = 1$, $\lambda = 0.3\omega_e$, $E = 0.1\omega_e$, $\omega_c = 10\omega_e$, $\Gamma = 0.1\omega_e$, for (a); $\omega_c = \omega_e$, $\Gamma = 0.1\omega_e$ for (b); $\omega_c = 10\omega_e$, $\Gamma = 3\omega_e$ for (c); $\omega_c = \omega_e$, $\Gamma = \omega_e$ for (d); $\omega_c = \omega_e$, $\Gamma = 2\omega_e$ for (e); $\omega_c = \omega_e$, $\Gamma = 3\omega_e$ for (f).

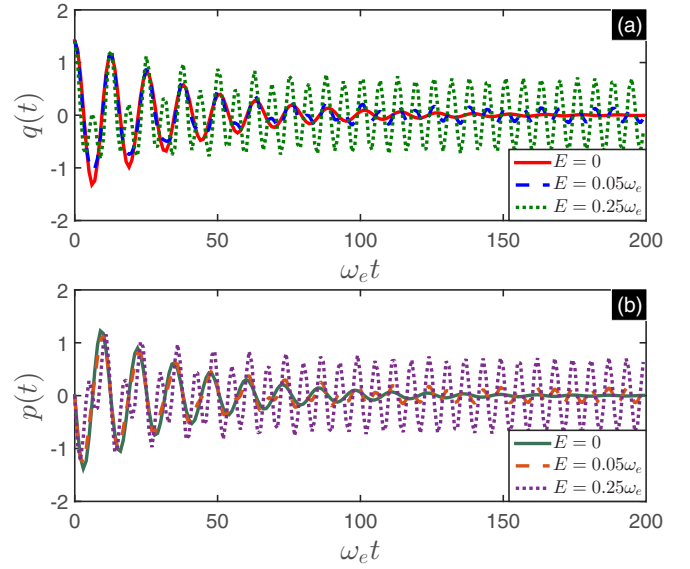


FIG. 6. Evolution in time of the expectation value of (a) position and (b) momentum [see Eq. (37)]. The different lines correspond to different values of the electric field intensity: $E = 0$ (solid line), $E = 0.05\omega_e$ (dashed line), $E = 0.25\omega_e$ (dotted line); the other parameters are $\Gamma = 0.05\omega_e$, $\lambda = 0.2\omega_e$, and $\omega_c = 0.5\omega_e$, whereas as initial conditions we set $\sqrt{\hbar}/2M_0\omega_c q(0) = 1$, $p(0)/\sqrt{\hbar M_0\omega_c} = 0$; the expectation values of position and momentum are expressed in units of $\sqrt{\hbar}/M_0\omega_c$ and $\sqrt{\hbar M_0\omega_c}$, respectively.

from Eq. (20),

$$q(t) = \text{Tr}_S[\hat{q}\rho_S(t)], \quad p(t) = \text{Tr}_S[\hat{p}\rho_S(t)]. \quad (37)$$

The evolution of the position variance $\sigma_{q^2}(t) = \text{Tr}_S[\hat{q}^2\rho_S(t)] - q^2(t)$ is obtained by squaring Eq. (37) and taking the expectation value, and similarly for the momentum variance $\sigma_{p^2}(t) = \text{Tr}_S[\hat{p}^2\rho_S(t)] - p^2(t)$ and the position-momentum covariance $\sigma_{qp}(t) = \text{Tr}_S\{[\hat{q}, \hat{p}]\rho_S(t)\}/2 - q(t)p(t)$.

First, in Figs. 6(a) and 6(b) we show the time evolution of the expectation values of position and momentum, respectively, for different values of the electric field strength E . In both cases and for a zero value of E , we find the expectation possessing decaying oscillations until approaching the asymptotic value zero. On the other hand, the introduction of coupling with the electric field decelerates the relaxation process of both quantities. The higher the value of E , the faster is the decay. The coupling with the electric field brings a further contribution to the Brownian particle due to its coupling with the environment. Indeed, referring to the master equation (20), it is clear how this feature can be traced back to the changes in the coherence coefficient $\phi(t)$, which now depends on $E(t)$.

Now, let us move our numerical analysis to the elements of the system covariance matrix, which, as said, completes the description of the reduced observables if we restrict ourselves to Gaussian states. In Figs. 7(a)–7(c), we show the evolution of $\sigma_{q^2}(t)$, $\sigma_{p^2}(t)$, and $\sigma_{qp}(t)$, respectively, for different values of E . Once again, we observe the relaxation toward the asymptotic value is faster when the electric field is strong. The coupling with the electric field accelerates the dissipation of the open system. In addition, the whole evolution of $\sigma_{qp}(t)$ is not modified qualitatively. Master equation (20) implies that the

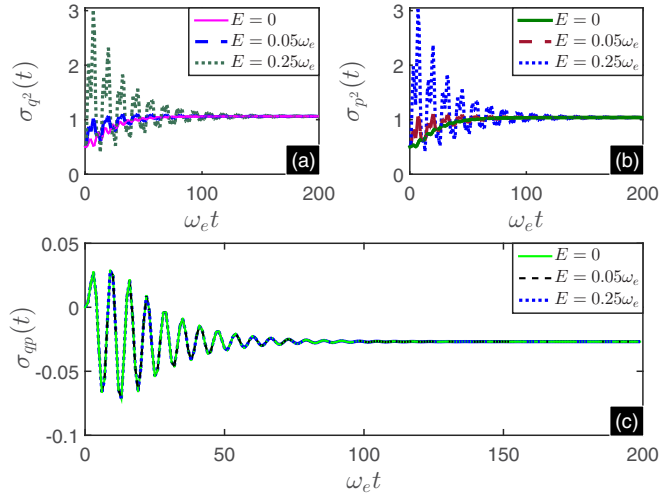


FIG. 7. Evolution in time of the elements of the covariance matrix: Variance of the position $\sigma_{q^2}(t)$ in (a), variance of the momentum $\sigma_{p^2}(t)$ in (b), and position-momentum covariance $\sigma_{qp}(t)$ in (c). The different lines correspond to $E = 0$ (solid line), $E = 0.05\omega_e$ (dashed line), and $E = 0.25\omega_e$ (dotted line). The other parameters are as in Fig. 6; the position variance is expressed in units of $\hbar/M_0\omega_e$, the momentum variance is expressed in units of $\hbar M_0\omega_e$, and the position-momentum covariance is expressed in units of \hbar .

Gaussian state is no longer the equilibrium state of the reduced dynamics, which instead exhibits a nonzero value of $\sigma_{qp}(t)$.

Recalling that the evolution of the momentum and position expectation values and covariances is calculated for a fixed initial condition, one might wonder if the feature observed depends on initial conditions. We verified numerically that the discussed asymptotic values do not depend on the initial conditions (at least, as long as one stays within the set of initial Gaussian states). Representative examples are given in Figs. 8(a) and 8(b) for the evolution of $\sigma_{q^2}(t)$ and $\sigma_{p^2}(t)$ with $E = 0$, and Figs. 8(c) and 8(d) with $E = 0.25\omega_e$, respectively. The system relaxes to a unique asymptotic state, for both cases. Moreover, from Figs. 8(c) and 8(d) we can observe that, for certain initial conditions, the position and momentum variances also relax to the asymptotic value in a nonmonotonic way, as we already observed for the expectation values in a nonzero electric field. Each variance can show even strong oscillations when its initial value is high enough and the oscillations are higher.

VII. COMPARISONS WITH THE APPROXIMATE METHODS

There are several methods with approximations in the literature to explore dissipative Brownian motion. In this section, we will compare the results by approximation with our exact one.

In the weak-coupling limit, the non-Markovian master equation can be derived perturbatively up to second order in system-environment couplings. Hence this master equation is available for weak system-environment couplings. Following the perturbation theory and after some algebra, we obtain a second-order time-convolutionless (TCL) non-Markovian

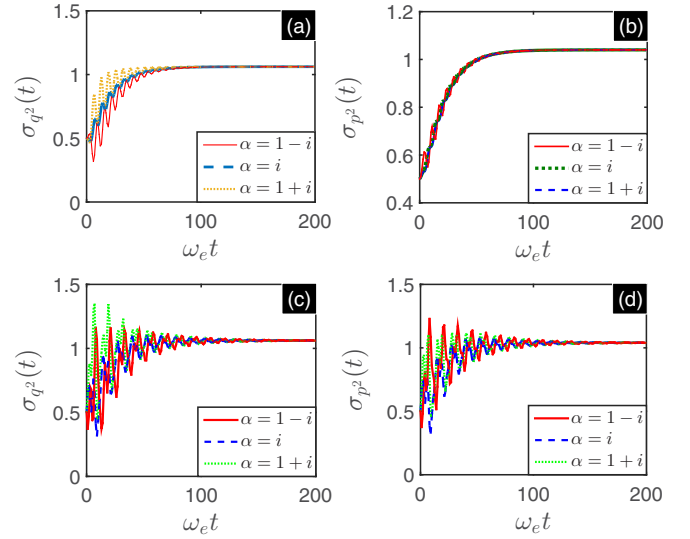


FIG. 8. Relaxation to the nonequilibrium stationary state of the variance for (a) and (b) $E = 0$ and (c) and (d) $E = 0.25\omega_e$. The different lines correspond to different initial coherent states: $\alpha = 1 - i$ (solid line), $\alpha = i$ (dashed line), and $\alpha = 1 + i$ (dotted line). The other parameters are the same as in Fig. 7.

master equation [42–45] for the system (3),

$$\begin{aligned} \dot{\rho}_S(t) = & -i[\hat{H}_{\omega c}(t), \rho_S(t)] \\ & + \gamma_1(t)(2\hat{a}\rho_S\hat{a}^\dagger - \hat{a}^\dagger\hat{a}\rho_S - \rho_S\hat{a}^\dagger\hat{a}) \\ & + \gamma_2(t)(\hat{a}\rho_S\hat{a}^\dagger + \hat{a}^\dagger\rho_S\hat{a} - \hat{a}^\dagger\hat{a}\rho_S - \rho_S\hat{a}^\dagger\hat{a}) \\ & + [\gamma_3^*(t)(2\hat{a}\rho_S\hat{a} - \hat{a}\hat{a}\rho_S - \rho_S\hat{a}\hat{a}) + \text{H.c.}], \end{aligned} \quad (38)$$

with the effective Hamiltonian

$$\hat{H}_{\omega c}(t) = \delta(t)\hat{a}^\dagger\hat{a} + [D(t)\hat{a}^2 + \phi(t)\hat{a} + \text{H.c.}], \quad (39)$$

where

$$\begin{aligned} D(t) &= \int_0^t d\tau \int d\omega J(\omega) e^{i\omega_c(t-\tau)} \sin \omega(\tau - t), \\ \delta(t) &= 2 \int_0^t d\tau \int d\omega J(\omega) \cos \omega_c(t - \tau) \sin \omega(\tau - t), \\ \phi(t) &= 2 \int_0^t d\tau \int d\omega J(\omega) \sin[\omega(\tau - t)] \Psi(\tau - t), \\ \gamma_1(t) &= \int_0^t d\tau \int d\omega J(\omega) \sin(\omega - \omega_c)(t - \tau), \\ \gamma_2(t) &= \int_0^t d\tau \int d\omega J(\omega) \sin(\omega + \omega_c)(t - \tau), \\ \gamma_3(t) &= \int_0^t d\tau \int d\omega J(\omega) e^{-i\omega_c(t-\tau)} \cos \omega(t - \tau). \end{aligned} \quad (40)$$

Here, $\Psi(t) = i \int_0^t d\tau E^*(\tau) e^{i\omega_c(t-\tau)} + \text{c.c.}$ Figure 9 shows a comparison of the exact and weak-coupling master equations with the bandwidth $\lambda = 0.3\omega_e$. We find that the results given by the weak-coupling master equation (38) are in good agreement with those obtained by the exact master equation (20) on any time scales [see Figs. 9(a) and 9(b)]. We therefore claim that for this range of parameters the TCL master equation gives

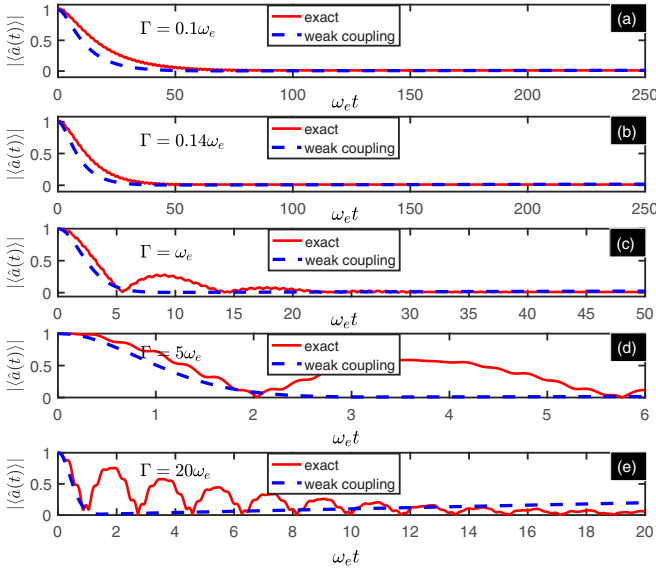


FIG. 9. Comparison of the exact non-rotating-wave and weak-coupling results for Brownian particle field amplitude $|\langle \hat{a}(t) \rangle|$ as a function of time in Ornstein-Uhlenbeck correlation (27). Red solid lines show the exact numerical results [see Eq. (20)]. Dashed lines are weak-coupling results [see Eq. (24)]. In all plots, we chose $\alpha = 1$, $\omega_c = \omega_e$, $E = 0.1\omega_e$, $\lambda = 0.3\omega_e$. The large deviation of (c)–(f) for the results from the exact non-rotating wave is caused by the strong coupling between the Brownian particle and environment, where the case is only valid in weak-coupling assumptions.

a better description for the dynamics, because it reflects all the qualitative characteristics of the exact results. In this case, the master equation in the weak-coupling limit gives a very good description of the dynamics. With a further increase of coupling strength in Fig. 9, clearly, the results given by the weak-coupling equation are in good agreement with those obtained by the exact one on a short-time scale, but they deviate from each other on a long-time scale [see Figs. 9(c)–9(e)]. Thus, in this case, the approximate method is not suitable to describe the dynamics.

VIII. QUANTUM NETWORK CONSISTING OF COUPLED CHARGED-BROWNIAN PARTICLES

In this section, we generalize these results to a more general network involving an arbitrary number of coupled quantum Brownian particles (CQBPs), whose Hamiltonian (see Fig. 10) is given by

$$\hat{H} = \hat{H}_S + \hat{H}_R + \hat{H}_{SR} + \hat{H}_E, \quad (41)$$

with

$$\begin{aligned} \hat{H}_S &= \sum_{m,n=1}^N \hbar \alpha_{mn} \hat{a}_m^\dagger \hat{a}_n, & \hat{H}_R &= \sum_k \hbar \omega_k \hat{b}_k^\dagger \hat{b}_k, \\ \hat{H}_{SR} &= \sum_{n,k} \hbar g_{n,k} (\hat{a}_n + \hat{a}_n^\dagger) (\hat{b}_k^\dagger + \hat{b}_k), \\ \hat{H}_E &= \sum_{n=1}^N \hbar E_n(t) \hat{a}_n^\dagger + \hbar E_n^*(t) \hat{a}_n, \end{aligned} \quad (42)$$

where α_{mn} are coupling constants between Brownian particles. The first equation is the free Hamiltonian of the N interacting

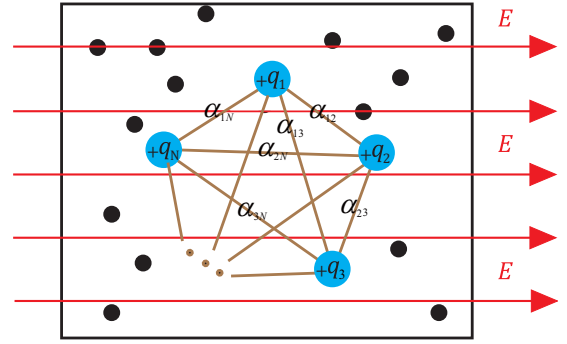


FIG. 10. Quantum network consisting of N mutually coupled charged-Brownian particles (coupling constants are α_{mn}) linearly interacting with the reservoir (modeled as harmonic oscillators with frequency ω_k). The blue circle represents the charged-Brownian oscillator, which is coupled to a large number of oscillators (the environment, shown by small black circles) interacting via the coupling constants $g_{n,k}$.

Brownian oscillators with frequency α_{mn} . The second term describes a general non-Markovian reservoir which is modeled as a collection of photonic modes (oscillators), where \hat{b}_k^\dagger and \hat{b}_k are the corresponding creation and annihilation operators of the k th photonic mode with frequency ω_k . $g_{n,k}$ are the reservoir mode-particle coupling constants. The fourth term denotes the interaction between the n th Brownian particle and the electric field. In this case, Eq. (8) reduces to

$$\begin{aligned} \frac{\partial \hat{a}_j(t)}{\partial t} &= -i \sum_{n=1}^N \alpha_{jn} \hat{a}_n(t) - i [\hat{B}_j(t) + \hat{B}_j^\dagger(t)] \\ &\quad - \sum_{m=1}^N \int_0^t d\tau K_{jm}(t-\tau) [\hat{a}_m(\tau) + \hat{a}_m^\dagger(\tau)] - i E_j(t), \end{aligned} \quad (43)$$

where the environment correlation function $K_{jm}(t) = f_{jm}(t) - f_{jm}^*(t)$ with $f_{jm}(t) = \sum_k g_{j,k} g_{m,k} e^{-i\omega_k t}$. According to the linearity of Eq. (43), we can write the operator $\hat{a}_m(t)$ as

$$\hat{a}_m(t) = \sum_{l_1=1}^N N_{ml_1}(t) \hat{a}_{l_1}(0) + \sum_{l_2=1}^N M_{ml_2}(t) \hat{a}_{l_2}^\dagger(0) + \hat{P}_m(t), \quad (44)$$

with the initial values $N_{ml}(0) = \delta_{ml}$, $M_{ml}(0) = 0$, and $\hat{P}_m(0) = 0$. The time-dependent coefficients satisfy the matrix differential equations,

$$\begin{aligned} \dot{N}(t) &= -i\alpha N(t) - \int_0^t dt K(t-\tau) [N(\tau) + M^*(\tau)], \\ \dot{M}(t) &= -i\alpha M(t) - \int_0^t dt K(t-\tau) [N^*(\tau) + M(\tau)], \\ \dot{P}(t) &= -i\alpha P(t) - \int_0^t dt K(t-\tau) [\hat{P}^*(\tau) + \hat{P}(\tau)] \\ &\quad - i\hat{B}(t) - \hat{B}^\dagger(t) - iE(t), \end{aligned} \quad (45)$$

where coefficient matrices $\hat{P}(t) = \hat{P}(t)_{N \times 1}$, $\hat{B}(t) = B(t)_{N \times 1}$ with $\hat{B}_m(t) = -i \sum_k (g_{m,k})^* e^{-i\omega_k t} \hat{b}_k(0)$, $E(t) = E(t)_{N \times 1}$. By solving the coupled Green's function equation (45), we can

obtain the complete information of the coupled-Brownian particles. It is particularly useful in the derivations of the exact master equation for the CQBP, achieved by completely integrating out the environmental degrees of freedom. Applications of the CQBP exact master equation cover various topics, such as quantum decoherence, the quantum-to-classical transition, and quantum measurement theory.

IX. DISCUSSION AND CONCLUSION

In summary, we have derived a non-Markovian master equation for a charged-Brownian particle in one dimension in an electric field and subject to a thermal reservoir. We find the non-Markovian dynamics governed by the master equation contains both time-dependent coefficients and coherent terms, which manifest the effects of the environment and the driving electric fields, respectively. We derive a current equation including a source coming from the driving fields, transient current from the system flowing into the environment, and the two-photon current from the non-rotating-wave term. Comparisons with the results given by second-order Born and Markovian approximations are made. We find that the latter two methods cannot exactly describe the system dynamics in the strong system-environment coupling regime. The presented results are generalized to a more general quantum network involving an arbitrary number of coupled-Brownian particles coupled to thermal reservoirs.

In experiments, the non-Markovian quantum Brownian motion in electric fields describes the forced oscillation of Brownian particles containing all feedback of the non-Markovian environment on quantum systems, which might be realized by a cold-atom Brownian motor in optical lattices [46], hard-sphere-plus-dipolar Brownian colloidal system [47], and optical tweezer experiments [48] as well as optically driven Brownian particles [49]. The electric fields may enter the system via a vector potential. In this sense, the prediction presented here is observable within the current technology.

Applications of our theory to a variety of physically relevant systems as well as its extension to a wide class of open quantum system, e.g., nonlinear coupling with the environments, deserve future investigations.

ACKNOWLEDGMENT

This work is supported by National Natural Science Foundation of China (NSFC) under Grants No. 11534002, No. 61475033, No. 11775048, and No. 11705025, China Postdoctoral Science Foundation under Grants No. 2016M600223 and No. 2017T100192, and the Fundamental Research Funds for the Central Universities under Grant No. 2412017QD005.

APPENDIX: DERIVATIONS OF EQ. (11)

1. Coupled modified Green's functions

Considering the initial conditions $\mathcal{N}(0) = 1$, $\mathcal{M}(0) = 0$, and $\hat{\mathcal{P}}(t) = 0$, we introduce two new coefficients $\mathcal{X}(t) = \mathcal{M}(t) + \mathcal{N}(t)$ with the initial condition $\mathcal{X}(0) = 1$, and $\mathcal{Y}(t) = \mathcal{M}(t) - \mathcal{N}(t)$ with the initial condition $\mathcal{Y}(0) = -1$. Then we

can obtain the evolution equation for $\mathcal{Y}(t)$ as follows,

$$\frac{d}{dt}\mathcal{Y}(t) = -i\omega_c\mathcal{Y}(t) - \int_0^t d\tau[\mathcal{Y}(\tau) - \mathcal{Y}^*(\tau)]\mathcal{K}(t - \tau). \quad (\text{A1})$$

Introducing $\mathcal{Z}(t) = \frac{1}{2}[\mathcal{Y}(t) + \mathcal{Y}^*(t)]$ with the initial condition $\mathcal{Z}(0) = -1$ and $\mathcal{W}(t) = \frac{1}{2i}[\mathcal{Y}(t) - \mathcal{Y}^*(t)]$ with the initial condition $\mathcal{W}(0) = 0$, the evolution equation of $\mathcal{Z}(t)$ and $\mathcal{W}(t)$ can be obtained,

$$\begin{aligned} \frac{d}{dt}\mathcal{Z}(t) &= \omega_c\mathcal{W}(t) - 2i \int_0^t d\tau\mathcal{W}(\tau)\mathcal{K}(t - \tau), \\ \frac{d}{dt}\mathcal{W}(t) &= -\omega_c\mathcal{Z}(t). \end{aligned} \quad (\text{A2})$$

The Laplace transformation for Eq. (A2) can be obtained as follows,

$$\begin{aligned} s\mathcal{Z}(s) + 1 &= \omega_c\mathcal{W}(s) - 2i\mathcal{W}(s)\mathcal{K}(s), \\ s\mathcal{W}(s) &= -\omega_c\mathcal{Z}(s). \end{aligned} \quad (\text{A3})$$

Solving Eq. (A3), we obtain

$$\begin{aligned} \mathcal{Z}(s) &= -\frac{s}{\omega_c^2 + s^2 - 2i\omega_c\mathcal{K}(s)}, \\ \mathcal{W}(s) &= \frac{\omega_c}{\omega_c^2 + s^2 - 2i\omega_c\mathcal{K}(s)}. \end{aligned} \quad (\text{A4})$$

With the same method, we can obtain the evolution equations for $\mathcal{X}(t)$ and $\mathcal{X}^*(t)$,

$$\frac{d}{dt}\mathcal{X}(t) = -i\omega_c\mathcal{X}(t) - \int_0^t d\tau[\mathcal{X}(\tau) + \mathcal{X}^*(\tau)]\mathcal{K}(t - \tau). \quad (\text{A5})$$

Introducing $\mathcal{C}(t) = \frac{1}{2}[\mathcal{X}(t) + \mathcal{X}^*(t)]$ with the initial condition $\mathcal{C}(0) = 1$ and $\mathcal{D}(t) = \frac{1}{2i}[\mathcal{X}(t) - \mathcal{X}^*(t)]$ with the initial condition $\mathcal{D}(0) = 0$, the evolution equation of $\mathcal{C}(t)$ and $\mathcal{D}(t)$ can be obtained,

$$\begin{aligned} \frac{d}{dt}\mathcal{C}(t) &= \omega_c\mathcal{D}(t), \\ \frac{d}{dt}\mathcal{D}(t) &= -\omega_c\mathcal{C}(t) + 2i \int_0^t d\tau\mathcal{C}(\tau)\mathcal{K}(t - \tau). \end{aligned} \quad (\text{A6})$$

The Laplace transformation for Eq. (A6) leads to

$$\begin{aligned} s\mathcal{C}(s) - 1 &= \omega_c\mathcal{D}(s), \\ s\mathcal{D}(s) &= -\omega_c\mathcal{C}(s) + 2i\mathcal{C}(s)\mathcal{K}(s). \end{aligned} \quad (\text{A7})$$

Solving Eq. (A7), we obtain

$$\begin{aligned} \mathcal{C}(s) &= \frac{s}{\omega_c^2 + s^2 - 2i\omega_c\mathcal{K}(s)}, \\ \mathcal{D}(s) &= -\frac{\omega_c - 2i\mathcal{K}(s)}{\omega_c^2 + s^2 - 2i\omega_c\mathcal{K}(s)}. \end{aligned} \quad (\text{A8})$$

Collecting all these together, we get

$$\begin{aligned} \mathcal{M}(t) &= \frac{1}{2}[[\mathcal{C}(t) + \mathcal{Z}(t)] + i[\mathcal{D}(t) + \mathcal{W}(t)]], \\ \mathcal{N}(t) &= \frac{1}{2}[[\mathcal{C}(t) - \mathcal{Z}(t)] + i[\mathcal{D}(t) - \mathcal{W}(t)]]. \end{aligned} \quad (\text{A9})$$

2. Solutions of nonhomogeneous Green's operator equation

If we set $\hat{Q}(t) = \frac{1}{2}[\hat{P}(t) + \hat{P}^\dagger(t)]$ and $\hat{R}(t) = \frac{1}{2i}[\hat{P}(t) - \hat{P}^\dagger(t)]$, we obtain evolution equations of $\hat{Q}(t)$ and $\hat{R}(t)$ as follows,

$$\begin{aligned} \frac{d}{dt}\hat{Q}(t) &= \omega_c\hat{R}(t) + E_i(t), \\ \frac{d}{dt}\hat{R}(t) &= -\omega_c\hat{Q}(t) + 2i\int_0^t d\tau\hat{Q}(\tau)\mathcal{K}(t-\tau) \\ &\quad -\hat{B}(t) - \hat{B}^\dagger(t) - E_r(t), \end{aligned} \quad (\text{A10})$$

where $E_r(t) = \frac{1}{2}[E^*(t) + E(t)]$ and $E_i(t) = \frac{i}{2}[E^*(t) - E(t)]$ are the real and imaginary parts of $E(t)$, respectively. The Laplace transformation for the Eq. (A10) can be obtained

$$\begin{aligned} s\hat{Q}(s) &= \omega_c\hat{R}(s) + E_i(s), \\ s\hat{R}(s) &= -\omega_c\hat{Q}(s) + 2i\hat{Q}(s)\mathcal{K}(s) - \hat{B}(s) - \hat{B}^\dagger(s) - E_r(s). \end{aligned} \quad (\text{A11})$$

Solving Eq. (A11), we obtain $\hat{Q}(s)$ and $\hat{R}(s)$,

$$\begin{aligned} \hat{Q}(s) &= \frac{sE_i(s) - [E_r(s) + \hat{B}(s) + \hat{B}^\dagger(s)]\omega_c}{s^2 + \omega_c[\omega_c - 2i\mathcal{K}(s)]}, \\ \hat{R}(s) &= \frac{-[E_r(s) + \hat{B}(s) + \hat{B}^\dagger(s)]s - E_i(s)[\omega_c - 2i\mathcal{K}(s)]}{s^2 + \omega_c[\omega_c - 2i\mathcal{K}(s)]}. \end{aligned} \quad (\text{A12})$$

Comparing with Eqs. (A4), (A8), (A9), and (A12), we obtain

$$\hat{P}(s) = -i[\mathcal{N}(s) - \mathcal{M}(s)][\hat{B}(s) + \hat{B}^\dagger(s)] + \mathcal{U}(s), \quad (\text{A13})$$

with

$$\mathcal{U}(s) = iE_r(s)[\mathcal{M}(s) - \mathcal{N}(s)] - E_i(s)[\mathcal{M}^*(s) - \mathcal{N}(s)]. \quad (\text{A14})$$

With an inverse Laplace transformation to Eq. (A13), we can obtain Eq. (11).

-
- [1] I. Buluta, S. Ashhab, and F. Nori, Natural and artificial atoms for quantum computation, *Rep. Prog. Phys.* **74**, 104401 (2011).
- [2] J. Q. You and F. Nori, Superconducting circuits and quantum information, *Phys. Today* **58** (11), 42 (2005); Atomic physics and quantum optics using superconducting circuits, *Nature (London)* **474**, 589 (2011).
- [3] H. P. Breuer, E. M. Laine, J. Piilo, and B. Vacchini, *Colloquium: Non-Markovian dynamics in open quantum systems*, *Rev. Mod. Phys.* **88**, 021002 (2016).
- [4] I. de Vega and D. Alonso, Dynamics of non-Markovian open quantum systems, *Rev. Mod. Phys.* **89**, 015001 (2017).
- [5] D. Chruściński and A. Kossakowski, Non-Markovian Quantum Dynamics: Local Versus Nonlocal, *Phys. Rev. Lett.* **104**, 070406 (2010).
- [6] B. H. Liu, L. Li, Y. F. Huang, C. F. Li, G. C. Guo, E. M. Laine, H. P. Breuer, and J. Piilo, Experimental control of the transition from Markovian to non-Markovian dynamics of open quantum systems, *Nat. Phys.* **7**, 931 (2011).
- [7] K. H. Madsen, S. Ates, T. Lund-Hansen, A. Löffler, S. Reitzenstein, A. Forchel, and P. Lodahl, Observation of Non-Markovian Dynamics of a Single Quantum Dot in a Micropillar Cavity, *Phys. Rev. Lett.* **106**, 233601 (2011).
- [8] S. Gröblacher, A. Trubarov, N. Prigge, G. D. Cole, M. Aspelmeyer, and J. Eisert, Observation of non-Markovian micromechanical Brownian motion, *Nat. Commun.* **6**, 7606 (2015).
- [9] H. P. Breuer and F. Petruccione, *The Theory of Open Quantum Systems* (Oxford University, Oxford, UK, 2002).
- [10] C. W. Gardiner and P. Zoller, *Quantum Noise*, 3rd ed. (Springer, Berlin, 2004).
- [11] U. Weiss, *Quantum Dissipative Systems*, 3rd ed. (World Scientific, Singapore, 2008).
- [12] A. J. Leggett, S. Chakravarty, A. T. Dorsey, M. P. A. Fisher, A. Garg, and W. Zwerger, Dynamics of the dissipative two-state system, *Rev. Mod. Phys.* **59**, 1 (1987).
- [13] F. Haake and R. Reibold, Strong damping and low-temperature anomalies for the harmonic oscillator, *Phys. Rev. A* **32**, 2462 (1985).
- [14] B. L. Hu, J. P. Paz, and Y. Zhang, Quantum Brownian motion in a general environment: Exact master equation with nonlocal dissipation and colored noise, *Phys. Rev. D* **45**, 2843 (1992).
- [15] J. J. Halliwell and T. Yu, Alternative derivation of the Hu-Paz-Zhang master equation of quantum Brownian motion, *Phys. Rev. D* **53**, 2012 (1996).
- [16] G. W. Ford and R. F. O'Connell, Exact solution of the Hu-Paz-Zhang master equation, *Phys. Rev. D* **64**, 105020 (2001).
- [17] R. P. Feynman and F. L. Vernon, The theory of a general quantum system interacting with a linear dissipative system, *Ann. Phys. (NY)* **24**, 118 (1963).
- [18] T. Yu, Non-Markovian quantum trajectories versus master equations: Finite-temperature heat bath, *Phys. Rev. A* **69**, 062107 (2004).
- [19] W. M. Zhang, P. Y. Lo, H. N. Xiong, M. W. Y. Tu, and F. Nori, General Non-Markovian Dynamics of Open Quantum Systems, *Phys. Rev. Lett.* **109**, 170402 (2012).
- [20] M. W. Y. Tu and W. M. Zhang, Non-Markovian decoherence theory for a double-dot charge qubit, *Phys. Rev. B* **78**, 235311 (2008).
- [21] H. Z. Shen, D. X. Li, S. L. Su, Y. H. Zhou, and X. X. Yi, Exact non-Markovian dynamics of qubits coupled to two interacting environments, *Phys. Rev. A* **96**, 033805 (2017).
- [22] K. W. Chang and C. K. Law, Non-Markovian master equation for a damped oscillator with time-varying parameters, *Phys. Rev. A* **81**, 052105 (2010).
- [23] H. Z. Shen, X. Q. Shao, G. C. Wang, X. L. Zhao, and X. X. Yi, Quantum phase transition in a coupled two-level system embedded in anisotropic three-dimensional photonic crystals, *Phys. Rev. E* **93**, 012107 (2016).
- [24] H. T. Tan and W. M. Zhang, Non-Markovian dynamics of an open quantum system with initial system-reservoir correlations: A nanocavity coupled to a coupled-resonator optical waveguide, *Phys. Rev. A* **83**, 032102 (2011).
- [25] H. Z. Shen, D. X. Li, and X. X. Yi, Non-Markovian linear response theory for quantum open systems and its applications, *Phys. Rev. E* **95**, 012156 (2017).

- [26] J. P. Paz and A. J. Roncaglia, Dynamical phases for the evolution of the entanglement between two oscillators coupled to the same environment, *Phys. Rev. A* **79**, 032102 (2009).
- [27] H. Z. Shen, M. Qin, and X. X. Yi, Single-photon storing in coupled non-Markovian atom-cavity system, *Phys. Rev. A* **88**, 033835 (2013).
- [28] T. Niemczyk, F. Deppe, H. Huebl, E. P. Menzel, F. Hocke, M. J. Schwarz, J. J. Garcia-Ripoll, D. Zueco, T. Hümmer, E. Solano, A. Marx, and R. Gross, Circuit quantum electrodynamics in the ultrastrong-coupling regime, *Nat. Phys.* **6**, 772 (2010); A. Wallraff, D. I. Schuster, A. Blais, L. Frunzio, R. S. Huang, J. Majer, S. Kumar, S. M. Girvin, and R. J. Schoelkopf, Strong coupling of a single photon to a superconducting qubit using circuit quantum electrodynamics, *Nature (London)* **431**, 162 (2004); P. Forn Diaz, J. Lisenfeld, D. Marcos, J. J. Garcia-Ripoll, E. Solano, C. J. P. M. Harmans, and J. E. Mooij, Observation of the Bloch-Siegert Shift in a Qubit-Oscillator System in the Ultrastrong Coupling Regime, *Phys. Rev. Lett.* **105**, 237001 (2010).
- [29] T. B. Batalhão, G. D. de Moraes Neto, M. A. de Ponte, and M. H. Y. Moussa, Nonperturbative approach to system-reservoir dynamics in the strong-coupling regime and non-Markovian dynamics, *Phys. Rev. A* **90**, 032105 (2014).
- [30] M. Carlesso and A. Bassi, Adjoint master equation for quantum Brownian motion, *Phys. Rev. A* **95**, 052119 (2017).
- [31] A. Lampo, S. H. Lim, J. Wehr, P. Massignan, and M. Lewenstein, Lindblad model of quantum Brownian motion, *Phys. Rev. A* **94**, 042123 (2016).
- [32] L. Ferialdi and A. Smirne, Momentum coupling in non-Markovian quantum Brownian motion, *Phys. Rev. A* **96**, 012109 (2017).
- [33] D. Boyanovsky and D. Jasnow, Heisenberg-Langevin vs quantum master equation, *Phys. Rev. A* **96**, 062108 (2017).
- [34] C. U. Lei and W. M. Zhang, A quantum photonic dissipative transport theory, *Ann. Phys. (NY)* **327**, 1408 (2012).
- [35] L. P. Kadanoff and G. Baym, *Quantum Statistical Mechanics* (Benjamin, New York, 1962).
- [36] A. Shabani, M. Mohseni, H. Rabitz, and S. Lloyd, Efficient estimation of energy transfer efficiency in light-harvesting complexes, *Phys. Rev. E* **86**, 011915 (2012).
- [37] M. Mohseni, A. Shabani, S. Lloyd, Y. Omar, and H. Rabitz, Geometrical effects on energy transfer in disordered open quantum systems, *J. Chem. Phys.* **138**, 204309 (2013).
- [38] C. M. Van Vliet, *Equilibrium and Non-equilibrium Statistical Mechanics* (World Scientific, Singapore, 2008).
- [39] K. Goldstein and D. A. Lowe, A note on α -vacua and interacting field theory in de Sitter space, *Nucl. Phys. B* **669**, 325 (2003).
- [40] G. E. Uhlenbeck and L. S. Ornstein, On the theory of the Brownian motion, *Phys. Rev.* **36**, 823 (1930).
- [41] D. T. Gillespie, Exact numerical simulation of the Ornstein-Uhlenbeck process and its integral, *Phys. Rev. E* **54**, 2084 (1996).
- [42] G. Guarnieri, C. Uchiyama, and B. Vacchini, Energy backflow and non-Markovian dynamics, *Phys. Rev. A* **93**, 012118 (2016).
- [43] J. Piilo, S. Maniscalco, and K. A. Suominen, Quantum Brownian motion for periodic coupling to an Ohmic bath, *Phys. Rev. A* **75**, 032105 (2007).
- [44] J. Paavola, J. Piilo, K. A. Suominen, and S. Maniscalco, Environment-dependent dissipation in quantum Brownian motion, *Phys. Rev. A* **79**, 052120 (2009).
- [45] G. Guarnieri, J. Nokkala, R. Schmidt, S. Maniscalco, and B. Vacchini, Energy backflow in strongly coupled non-Markovian continuous-variable systems, *Phys. Rev. A* **94**, 062101 (2016).
- [46] M. Zelan, H. Hagman, G. Labaigt, S. Jonsell, and C. M. Dion, Experimental measurement of efficiency and transport coherence of a cold-atom Brownian motor in optical lattices, *Phys. Rev. E* **83**, 020102(R) (2011).
- [47] H. D. Newman and A. Yethiraj, Clusters in sedimentation equilibrium for an experimental hard-sphere-plus-dipolar Brownian colloidal system, *Sci. Rep.* **5**, 13572 (2015).
- [48] M. Grimm, T. Franosch, and S. Jeney, High-resolution detection of Brownian motion for quantitative optical tweezers experiments, *Phys. Rev. E* **86**, 021912 (2012).
- [49] A. Imparato, L. Peliti, G. Pesce, G. Rusciano, and A. Sasso, Work and heat probability distribution of an optically driven Brownian particle: Theory and experiments, *Phys. Rev. E* **76**, 050101(R) (2007).